

10ème Congrès Français d'Acoustique

Lyon, 12-16 Avril 2010

Example of structure modeling and analysis of ultrasound scattering for trabecular bone.

Janusz Wojcik¹, Jerzy Litniewski¹, Andrzej Nowicki¹

¹Institute of the Fundamental Technological Research of the Polish Academy of Sciences, Adolfa Pawińskiego Str. 5B, 02-106 Warsaw, Poland

jwojcik@ippt.gov.pl

Trabecular bone consists of trabeculae which mechanical properties differ significantly from the surrounding marrow and therefore the ultrasonic wave is strongly scattered within the bone structure. The aim of the presented paper was the evaluation of the contribution of the first, second and higher order scattering (multiple scattering) into total scattering of ultrasounds in the trabecular bone. The scattering due to interconnections between thick trabeculae, usually neglected in trabecular bone models, has been also studied. The basic element in our model of trabecular bone was an elastic cylinder with finite-length and varying diameter and orientation. The applied model was taking into account variation of elements size and spatial configuration. The field scattered on the bone model was evaluated by solving numerically the integral form of the Sturm-Liouville equation that describes scalar wave in inhomogeneous media. For the calculated scattered fields the effective cross-sections as well as the Broadband Ultrasonic Backscatter (BUB) were determined. The influence of the absorption on scattering coefficients was demonstrate. The results allowed to conclude that within the frequency range from 0.5 to 1.5 MHz the contribution of the second order scattering to the effective backscattering cross-section is at least 500 times lower than the one due to the first order scattering. BUB, calculated under the same assumptions, is 20 times lower. Above the 1.5 MHz the fast growth of the BUB, calculated for the second order scattering, occurs.

1 Introduction

The evaluation of bone strength requires not only the knowledge of its mean density but also of its microscopic structure. The ultrasound signals that have been scattered in trabecular bone contain information of the properties of the bone structure, and hence the analysis of the backscatter could be useful in assessment of the microscopic architecture of the bone. It has been demonstrated that the use of the backscattering models of bone enabled an assessment of some micro-structural characteristics from the experimental data.

Starting from Wear's work [1], the best of the authors' knowledge almost all of the reported bone scattering models assumed, not precisely speaking the Born approximation, and consequently the multiple scattering within the bone trabeculae, was neglected. Trabecular bone consists of trabeculae whose mechanical properties differ significantly from the surrounding marrow and therefore the ultrasonic wave is strongly scattered. The work of Bossey et al.[2] presents analytically advanced approach. The scattering structure corresponds to the real one. Unfortunately this approach does not enable determination of the influence of multiple scattering on total The field. The Wear's [3] work contains the review of methods and problems of bone sonometry.

The aim of the presented paper was the evaluation of the contribution of the first, second and higher order scattering (multiple scattering) into total scattering of the ultrasounds in the trabecular bone. The scattering, due to interconnections between thick trabeculae, usually

neglected in trabecular bone models, has been also studied. Our model is fully scaled.

The basic element in our model of trabecular bone was an elastic cylinder with varying finite-length and diameter as well as orientation. The density and speed of sound were similar to those of the bone tissue. The cylinder was applied in building of the multi-element structures, similar to the architecture of the trabecular bone, taking into account variation of elements size and spatial configuration. The field scattered on the bone model was evaluated by solving numerically the integral form of the Sturm-Liouville equation in the version that describes longitudinal wave in inhomogeneous and lossy media.

For the calculated scattered fields the effective cross-sections as well as the Broadband Ultrasonic Backscatter (BUB), directly related to the detected echo-signal level, were determined. Calculations were performed for the different absorption parameters and for the frequency ranging from 0.5 to 3 MHz.

2 Basic equations

The Lamé's equation for longitudinal (volumetric) disturbances in non-homogeneous, isotropic and stationary medium given in [4] can be rewritten in space-Fourier frequency domain as follows

$$g \nabla \cdot \left(\frac{\nabla C}{g} \right) + K^2 C = 0 \quad (1)$$
$$K^2 = K(\mathbf{x}, n)^2 \equiv \frac{n^2}{c^2 (1 - 2i(a(\mathbf{x}, n)/gc^2 n))}$$

$$C = \left(\lambda + 2\mu + 2 \frac{a(n)}{in} \right) \nabla \cdot \mathbf{u}_F = gc^2 \left(1 + 2 \frac{a(n)}{gc^2 in} \right) \nabla \cdot \mathbf{u}_F \quad (2)$$

Where $C = C(\mathbf{x}, n) = F[P(\mathbf{x}, t)]$, $\mathbf{u}_F(\mathbf{x}, n) = F[\mathbf{u}(\mathbf{x}, t)]$; $P = P(\mathbf{x}, t)$ is the normalized stress; $P \equiv \bar{P}/P_0$, P_0 is the reference pressure, $\mathbf{u} = \mathbf{u}(\mathbf{x}, t)$ is the normalized displacement vector; $\lambda + 2\mu = gc^2$, $\lambda = \lambda(\mathbf{x})$, $\mu = \mu(\mathbf{x})$ are the first and the second Lamé's constants; $g = g(\mathbf{x})$, $c = c(\mathbf{x})$ are respectively: normalized density and speed of the longitudinal (sound) waves, (\mathbf{x}, t) are normalized coordinates in space and time, whereas ∇ is the normalized nabla vector operator, symbol: \bullet denotes scalar product, $\Delta \equiv \nabla \cdot \nabla$ is the scalar Laplacian. The normalization was performed as follows: $g \equiv \bar{g}/g_0$, $c \equiv \bar{c}/c_0$, $\mathbf{u} \equiv K_0 \bar{\mathbf{u}}$, $\mathbf{x} \equiv K_0 \bar{\mathbf{x}}$, $t \equiv \omega_0 \bar{t}$, $\nabla \equiv \bar{\nabla}/K_0$. The dimensional variables and operators are accented; g_0 , c_0 are density and speed of sound in reference medium respectively (in our case - volume dominant reference), $\lambda_0 + 2\mu_0 = g_0 c_0^2$. It means that $c = 1$ and $g = 1$ for reference medium. The characteristic wave number K_0 and pulsation ω_0 are restricted by the relation: $K_0 c_0 = \omega_0$. $\omega_0 \equiv 2\pi/T_0$, where T_0 is reference time (e.g. Time window). A consequence of the applied normalization method is equality of non-dimensional pulsation $n \equiv \omega/\omega_0$ and frequency, and the wave number in dispersion less media $k(n) = \pm n$. In homogeneous regions of the medium $a(n) = a(\mathbf{x}, n)$; $a(\mathbf{x}, n)$ denotes spatial distribution of the small signal coefficient of absorption.

The investigation of the absorption influence on the wave propagation in many media (especially biological) require generalization of the constitutive relation $C = (\lambda + 2\mu - 2i\alpha_2 n) \nabla \cdot \mathbf{u}_F$ ($P = (\lambda + 2\mu + 2\alpha_2 \partial_t) \nabla \cdot \mathbf{u}$;

$\alpha_2 \equiv (\eta_b + 4\eta_{sh}/3)/2$; $\eta_{sh} \equiv \bar{\eta}_{sh} \omega_0 / g_0 c_0^2$; $\eta_b \equiv \bar{\eta}_b \omega_0 / g_0 c_0^2$ are normalized share and bulk viscosity's respectively) describing classically (viscous) absorbing media. We propose this generalization in the form given by Eq.2. For $a(n) = \alpha_2 n^2$ we obtain classically absorbing (viscous) media.

Simplification of the full Lamé's equation to the form given by Eq.1 depends on analytical properties of the assumed heterogeneity model (the assumption $\nabla \times \mathbf{u} = 0$ only is not sufficient for derivation of Eq.1). The next chapter will present a model of heterogeneous medium with step rise changing material parameters, for which $\Delta\mu = 0$ also on the surfaces of phase separation, despite the fact that $\nabla\mu \neq 0$ on these surfaces. We rewrite the Eq.(1) in the form of the Sturm-Liouville equation,

$$\begin{aligned} \Delta C + k^2 C &= V C + \mathbf{Q} \cdot \nabla C \\ k^2 &= k(n)^2 \equiv n^2 / (1 - 2i(a_0(n)/n)) \\ V &= V(\mathbf{x}, n) \equiv -(K(x, n)^2 - k(n)^2) \\ \mathbf{Q}(\mathbf{x}) &\equiv \nabla g / g \end{aligned} \quad (3)$$

Where $a_0(n)$ is the absorption coefficient of the reference medium.

3 Medium construction

We assume that reference homogeneous medium surrounds L regions v_l of space. The regions are bounded by surfaces s_l $l = 1, \dots, L$. We suppose that v_l are open sets in space, however $\bar{v}_l = v_l \cup s_l$ are closed. Each region \bar{v}_l is filled with homogeneous medium and its normalized density $g_l \neq 1$, as well as normalized speed of the longitudinal waves $c_l \neq 1$. The multiple-theory sum of the v_l sets describes the structure being submerged in reference medium. We assume that elements of structure do not cross in a sense of 3D measure of volume $d^3(\cdot)$ however they may wear tangential. $v = \bigcup_l v_l$, $s = \bigcup_l s_l$, $d^3(v_l \cap v_m) = 0$, $d^{2,1}(\bar{v}_l \cap \bar{v}_m) \neq 0$. Thus spatial distributions of sound speed, density and absorption coefficient have a form:

$$\begin{aligned} c(\mathbf{x})^2 &= 1 + \sum_l d c_l(\mathbf{x})^2 = 1 + \sum_l \chi_l (c_l^2 - 1) \\ g(\mathbf{x}) &= 1 + \sum_l d g_l(\mathbf{x}) = 1 + \sum_l \chi_l (g_l - 1) \\ a(\mathbf{x}, n) &= a_0(n) + \sum_l d a_l(\mathbf{x}, n) = a_0(n) + \sum_l \chi_l (a_l(n) - a_0(n)) \end{aligned} \quad (4)$$

where $d \dots$ denotes step rise of material parameters; $\chi_l \equiv \chi(\bar{v}_l)$ is the characteristic function of \bar{v}_l , $\chi = 1$ for $\mathbf{x} \in v_l$, $\chi = 0$ for $\mathbf{x} \notin \bar{v}_l$, $\chi = 1/2$ for $\mathbf{x} \in s_l$.

Neglect detailed discussion, we have

$$V = \sum_l \chi_l n^2 \left(\frac{1}{1 - 2i(a_0(n)/n)} - \frac{1}{c_l^2 (1 - 2i(a_l(n)/g_l c_l^2 n))} \right) \quad (5)$$

$$\begin{aligned} \mathbf{Q}(\mathbf{x}) &= \mathbf{Q}(\mathbf{x}) \mathbf{e}(\mathbf{x}) \delta(s) = \\ &= \left(\sum_l \sigma_l \left(\frac{1 - g_l}{(g_l + 1)/2} \right) \right) \mathbf{e}(\mathbf{x}) \delta(s) \end{aligned} \quad (6)$$

Vector $\mathbf{e}_l(\mathbf{x})$ is externally normal to s_l in $\mathbf{x} \in s_l$ and is unit. Because $\mathbf{e}(\mathbf{x}) = \{\mathbf{e}_l(\mathbf{x}) : \mathbf{e}_l \perp s_l, l = 1, \dots, L\}$ is a general field of the unit vectors being normal to the structure, then: $\delta(s_l) \mathbf{e}(\mathbf{x}) = \delta(s_l) \mathbf{e}_l(\mathbf{x})$ since for $\mathbf{x} \notin s_l$ $\delta(s_l) = 0$.

4 Scattering equations

For the assumed model of structure of medium the Eq.(3) becomes as follows

$$\Delta C + k^2 C = V C + \mathbf{Q} B \delta(s), \quad (7)$$

Where $B(\mathbf{x}, n) \equiv \mathbf{e}(\mathbf{x}) \cdot \nabla C(\mathbf{x}, n)$. The field B is determined only on surface s of the structure \bar{v} . Further, if it will not make misunderstanding the pulsation n will be neglected in the argument list. When transforming Eq.(7) into integral equation and using features of distributions $\delta(s)$ and $\chi(v)$ we obtain

$$\begin{aligned} C(\mathbf{x}) &= C^0(\mathbf{x}) - \int_v G(r(\mathbf{x}, \mathbf{x}')) V(\mathbf{x}') C(\mathbf{x}') dv \\ &\quad - \int_s G(r(\mathbf{x}, \mathbf{x}')) Q(\mathbf{x}') B(\mathbf{x}') ds \end{aligned} \quad (8)$$

Where $G(r, n) \equiv \exp(ik(n)r/4\pi r)$, $r = r(\mathbf{x}, \mathbf{x}') = |\mathbf{x} - \mathbf{x}'|$, $C^0(\mathbf{x}) \equiv C^0(\mathbf{x}, n)$ is a solution of Helmholtz equation in reference medium (incident field), $G(r(\mathbf{x}, \mathbf{x}')) = G(r(\mathbf{x}, \mathbf{x}'), n)$ is the Green function of the Helmholtz equation. Applying $\mathbf{e}(\mathbf{x}) \cdot \nabla$ to the both sides of Eq.(8) we get equation for the field B (acceleration).

$$B(\mathbf{x}) = B^0(\mathbf{x}) - \int_v \partial G(r(\mathbf{x}, \mathbf{x}')) V(\mathbf{x}') C(\mathbf{x}') dv - \int_s \partial G(r(\mathbf{x}, \mathbf{x}')) Q(\mathbf{x}') B(\mathbf{x}') ds \quad (9)$$

where: $B^0 = \mathbf{e} \cdot \nabla C^0$, $\partial G(r) \equiv \mathbf{e}(\mathbf{x}) \cdot \mathbf{e}(\mathbf{r}) \partial_r G$, $\mathbf{e}(\mathbf{r}) = \nabla r = \mathbf{r}/r$. The integrals in Eq.8,9 describe the scattering of incident field on potentials V and Q of the structure. It is sufficient to determine the equations for $\mathbf{x} \in \bar{v}$ in order to solve it. When the solution is substituted to the integrals in Eq.(8) it gives solution in whole medium.

By grouping the functions and their normal derivatives in vector function

$$\bar{C} \equiv \begin{pmatrix} C \\ B \end{pmatrix}, \bar{C}^0 \equiv \begin{pmatrix} C^0 \\ B^0 \end{pmatrix}, \bar{G} \equiv \begin{pmatrix} G \\ \partial G \end{pmatrix}, W \equiv \begin{pmatrix} V dv \\ Q ds \end{pmatrix} \quad (10)$$

and introducing the scattering field $E \equiv \bar{C} - \bar{C}^0$, we may rewrite Eqs.(8) and (9) in the compact form

$$(\mathbf{I} + \mathbf{GW})E = -E^0$$

$$\mathbf{GW} \bar{C} \equiv \int (\bar{G} \circ W) \bar{C} \quad (11)$$

where, the kernel of operator \mathbf{GW} is 2×2 matrices (matrix of matrices) determined by diadic vectors product signs by \circ , $E^0 = \mathbf{GW} \bar{C}^0$. \mathbf{I} is the identity operation $\mathbf{I}E(\mathbf{x}') = E(\mathbf{x})$. Equivalent form of the operator \mathbf{GW} is

$$\mathbf{GW} \equiv \begin{pmatrix} \int dv V G & \int ds Q G \\ \int dv V \partial G & \int ds Q \partial G \end{pmatrix} \quad (12)$$

Integration domains are clearly determined by dv and ds . Because $E = \sum_l \chi_l E_l$ then the operator

\mathbf{GW} can be presented as the sum of the cells $\mathbf{GW} = \bigcup_{l,m} \mathbf{GW}_{lm}$, where \mathbf{GW}_{lm} is given by Eq.(11) or (12)

for $W_m = \chi_m W$ and $\mathbf{x} \in \bar{v}_l$. For $\mathbf{x}, \mathbf{x}' \in \bar{v}_l$ and $\mathbf{x} = \mathbf{x}'$,

$\mathbf{GW}_{lm} = \mathbf{0}$ (no self interaction). We set $\mathbf{GW}_l \equiv \mathbf{GW}_{ll}$ for diagonal cells $l = m$.

5 Solution method

We seek the solution of Eq.(11) for $\mathbf{x} \in v$ in the form

$$E = \sum_l E_l^1 + R^2 \quad (13)$$

where E_l^1 is the solution of Eq.(11) in l -th element of the structure under the assumption that the only scattering field in \bar{v}_l is $E_l^0 = \chi_l E^0$ produced by incident field $\bar{C}_l^0 = \chi_l \bar{C}^0$, $E_l^0 = \mathbf{GW}_l \bar{C}_l^0$.

$$(\mathbf{I} + \mathbf{GW}_l)E_l^1 = -E_l^0 \quad (14)$$

$$E_l^1 = -\mathbf{H}_l E_l^0 = -\mathbf{H}_l \mathbf{GW}_l \bar{C}_l^0, \quad l = 1, \dots, L \quad (15)$$

where $\mathbf{H}_l \equiv (\mathbf{I} + \mathbf{GW}_l)^{-1}$ denotes inverse operator. The fields E_l^1 determine a field in medium in the first order of scattering (single scattering). The field E_l^0 represents first term in Neuman series obtained by iteration of the integral Equations (8) and (9). The reminder R^2 denotes a field in structure created due to interaction between structure elements in the second and higher orders of the scattering (multi-scattering). The R^2 satisfies equation

$$(\mathbf{I} + \mathbf{GW})R^2 = -\sum_l \mathbf{GW}_l \left(\sum_{m, m \neq l} E_m^1 \right) \quad (16)$$

$$E_m^1 = \mathbf{GW}_{lm} E_m^1$$

The field E_m^1 is calculated as the field from the m -th element *failing* on l -th element. Then we repeat the described above procedure. We suppose that $R^2 = \sum_l E_l^2 + R^3$ and E_l^2 satisfies (16) with source in

the form of l -th component on right side in (32). Then we have

$$E_l^2 = -\mathbf{H}_l \mathbf{GW}_l \sum_{m \neq l} E_m^1, \quad (17)$$

and after substitution $E_m^2 \rightarrow E_m^1$ R^3 satisfies Eq. (16).

Generally, in j -th order of the scattering $R^j = \sum_l E_l^j + R^{j+1}$

$$E_l^j = -\mathbf{H}_l \mathbf{GW}_l \sum_{m \neq l} E_m^{j-1} \quad (18)$$

Then in point \mathbf{x} of the medium the total j -th order component of the scattered field takes the form

$$E^j(\mathbf{x}) = -\sum_l \mathbf{GW}_l E_l^j(\mathbf{x}') \quad \mathbf{x}' \in \bar{v}_l \quad (19)$$

The total scattered field is given by sum of the $E^j(\mathbf{x})$.

We obtain the discrete (numerical) representation of the above procedure when W is replaced by the weight system $W(\zeta_l)$ for numerical integration's respect sampling structure vector $\mathbf{x} \rightarrow \mathbf{x}(\zeta_l)$. Where ζ_l is the sample index in l -th element of the scattered structure.

6 Trabecular bone model

The skeleton of the model of trabecular bone structure, applied in scattering field calculations, is presented in Figure 1:(a) left. One of skeleton structures parallel to the x - z plane (horizontal respect incident field) is shown in Figure 1: (a) right. The cylinder with diameter Φ and length d was adopted as the model of trabecular and bar. Each segment of the skeleton is the axis of cylinder.

The skeleton was obtained randomly by displacement of nodes in each layers of regular structure built of cuboids. The uniform probability was assumed for displacements. The horizontal structures were adjusted to new node positions. Then some elements were randomly eliminated from the structure. The structure is immersed in absorbing

(or not) fluid filler. The results are wary similar to those which were presented in [6] .

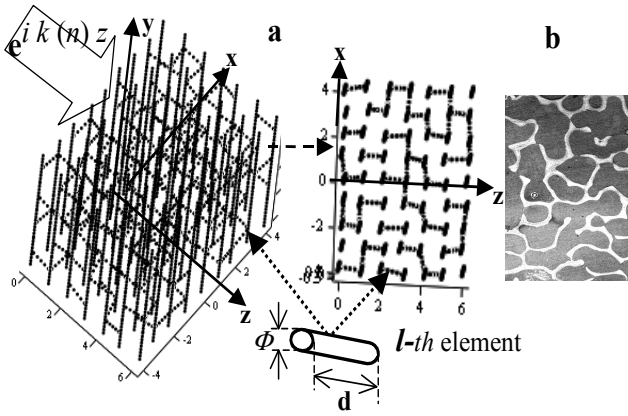


Figure 1 : (a) left: full skeleton of the trabecular bone model; right: one of horizontal substructures in the skeleton. (b) the cross-section of the real trabecular bone structure.

Our model is fully calibratable. The change of number of elements and their geometrical parameters enables various porosity. Changing probability distribution functions and their parameters we can create different statistical properties of the physical and geometrical parameters of the structure. It should be noted that in our model it is possible to change the shape of the elements, which fill the skeleton (cuboids, spheroids etc.).

7 Results

In the initial regular structure the cuboids dimensions are 2mm in the y direction and 1×1 mm in the x and z directions. For the nodes displacement the uniform probability was assumed in range $(-0.15; 0.15)$ mm. Also uniform probability for elimination of some elements from the structure were used.

Values of sound speed and densities of each trabecular were selected based on Gamma distribution. Maximum deviation from mean values 4000 m/s and 2000 kg/m³ was assumed as $\pm 5\%$. For trabecular, in y direction and in horizontal planes, mean values $\Phi=0.05$ and 0.04 mm with deviations $\pm 20\%$ and $\pm 25\%$ respectively, were assumed.

For surrounding medium (marrow - fluid filler) as well as surrounding space $g_0=1000\text{kg/m}^3$, $c_0=1500\text{m/s}$. The absorption parameters for fluid filler was $\alpha_1=(0.23;1.15;2.3) \cdot 10^{-4}$ Np/mHz, $a(n)=\alpha_1 c_0 |n|/2\pi$. Total number of elements (trabecular) was 443. Total dimensions are: $[-4;4]\text{mm}$ in x , $[-4;4]\text{mm}$ in y , $[0;6]\text{mm}$ in z direction (384mm^3).

The unit plane wave was assumed as incident field $C^0 = \exp(ik(\nu)z)$ $z \geq 0$, $\nu \in [0.5, 3]$ MHz with step 0.333 MHz. Dimensionless frequency is $n = 15, 16, \dots, 90$.

7.1 Scattering field distributions

Exemplary distributions of scattering fields for the absorption parameter $\alpha_1 = 2.3 \cdot 10^{-4}$ in subsequent orders and for selected frequencies were shown in Figure 2. Colors refers logarithmic scale of values. Contour of the scattering structure and its location is shown by red rectangle whereas

red narrow indicates direction of incident wave. The represented area is the rectangle with location $[-30, 20]$ mm in z direction and $[-15, 15]$ mm in x direction

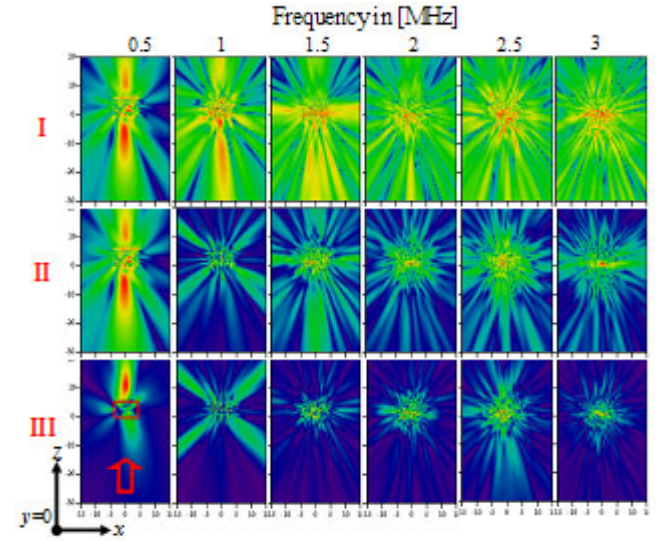


Figure 2 : Distributions of fields in subsequent orders of scattering in rows: I, II, III, while in function of frequency from 0.5 MHz to 3 MHz they are shown in columns.

7.2 Backscatter coefficients

We define substructures: horizontal (denoted by “h”) as a set of all trabecular that are situated in planes being parallel to the x - z plane, and vertical (denoted by “v”) as a set of all trabecular which are parallel to the y axis.

In Figure 3 S_I , S_{II} and S_{III} are the backscatter effective cross-section coefficients, that were obtained in subsequent orders of scattering (first-I, second-II, third-III) and in function of frequency ν . The influence of the absorption of the fluid filler on the effective cross-section in each order is presented. The plot p1 correspond to the last $\alpha_1=0.23 \cdot 10^{-4}$, p2 to the middle $\alpha_1=1.15 \cdot 10^{-4}$ and p3 to the $\alpha_1=2.3 \cdot 10^{-4}$ value of absorption parameter.

Square roots $\sqrt{S_I}$, $\sqrt{S_{II}}$, $\sqrt{S_{III}}$ were applied for better representation. Moreover, they are first range in respect to scattered field variations as well as invariants (as S_I , S_{II} , S_{III}) in respect to shape of the surface surrounding the scatter in hemispace. Then, the square root from the effective cross-section is a proper measure (norm) of the signal received by transducer placed close to the scatter. The backscatter (reflection) coefficients can be defined as follows:

$$\kappa_{I,II,III}(n) \equiv \frac{\sqrt{S_{I,II,III}(n)}}{\sqrt{\sigma_G}}, \quad (20)$$

where, for a given configuration, σ_G is the geometrical cross-section (area of normal projection of the scatter on surface that divides space into two hemispaces). In our case $\sigma_G = 64\text{mm}^2$. In the nearness of frequency $\nu = 1.5$ MHz, the estimated relations between values $S_I:S_{II}:S_{III}$, from Figure 3, are as 1:(0.001):(0.00001) for the case denoted by p1 and higher for the cases p1 and p2. In Figure 3 (left) the resonance for $\nu = 0.75$ MHz is observed and it is fully created by y substructure in which the trabecular length is 2mm. It corresponds to the resonance frequency. Similar analysis can be performed for other resonances using higher scattering orders.

In Figure 4: the contribution of substructures **h** and **y** to backscatter effective cross-sections for the case p1 in subsequent orders of scattering is presented. Let us notice the validity change of substructures in transition from the

first order to higher orders of scattering. It is visible in Figure 4 (left) and Figure 4(middle) (the transition occurs for $\nu > 1.6$ MHz).

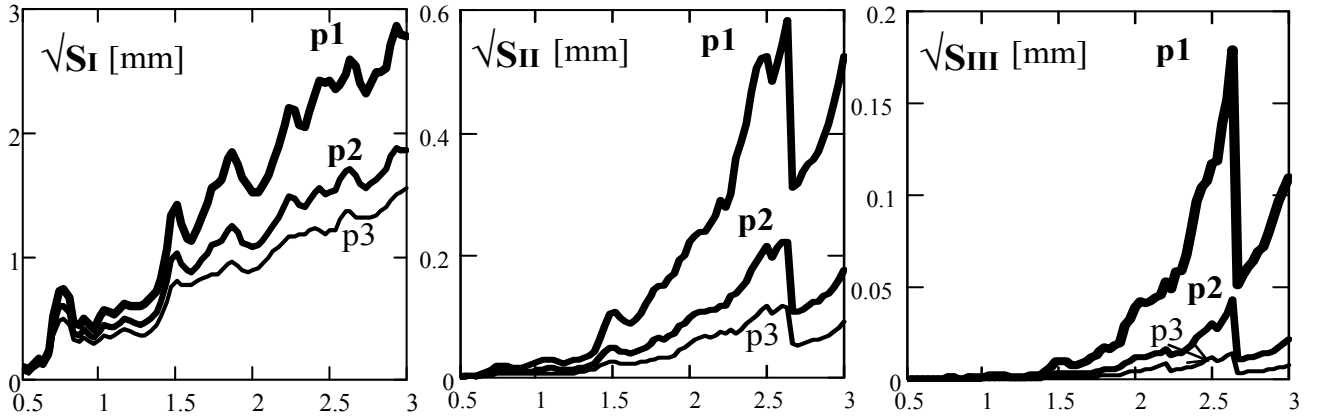


Figure 3: Backscatter effective cross-section decomposition in respect to scattering order, first- S_I , second- S_{II} and third- S_{III} . Plots p1, p2, p3 corresponds to the last-p1, middle-p2 and extreme-p3 value of absorption parameter. Frequency in MHz.

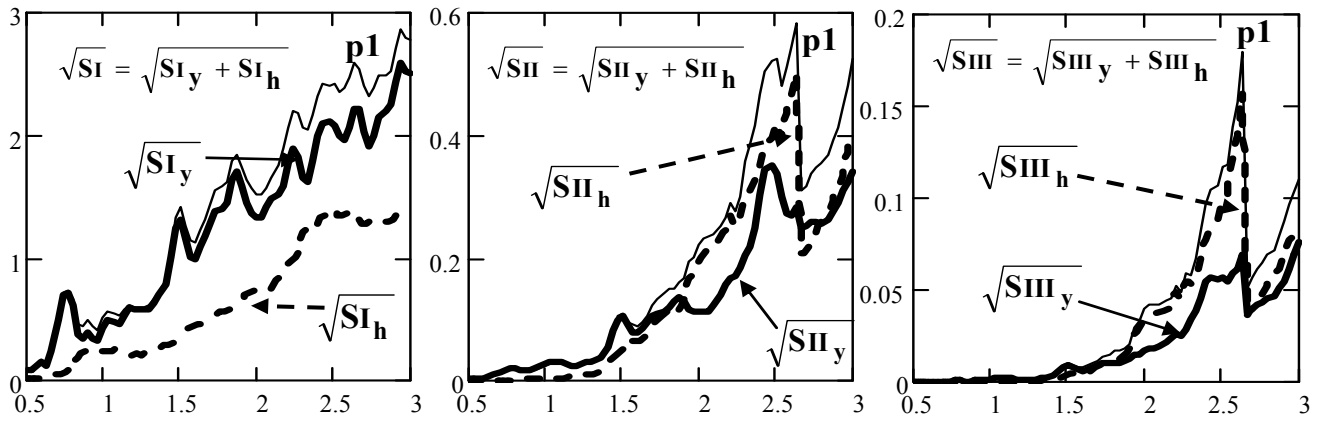


Figure 4: Contribution of substructures **h** and **y** in subsequent orders of scattering as well as in respect to frequency (in MHz) for the case p1 of the absorption parameter.

8 Conclusion

In space-frequency range the method of solving of longitudinal wave scattering equations has been developed. It is convergent for high potentials and multi-element structures in numerical applications.

The method is *accurate* in each order of scattering that means the calculated fields in subsequent order do not make *corrections* in scattering fields of former order. The Neuman's iteration of integral equations of scattering produce the asymptotically converged series (if it is converging); this means that each subsequent element of series *includes* improving accuracy corrections to former field elements for the selected structure element. The developed algorithm enables the analysis of the scattering field characteristics taking into account not only the scattering order but also the influence of selected substructures. The examples of this effect has been presented.

From the comparison of the plots p1, p2 and p3, on the left in Figure 3, the smoothing effect of the absorption on the relationship between the scattering coefficients and frequency/ the scattering coefficient dependence from frequency, results/follows/is seen.

Moreover, from the comparison of the relationship between p1, p2 and p3 for $\sqrt{S_I}$, $\sqrt{S_{II}}$, $\sqrt{S_{III}}$, the increase in the influence of absorption on the scattering process, in II and higher orders of scattering, is seen.

In the range up to 1.5 MHz the influence of higher scattering orders on characteristics of the first order in respect to the field is less than few percent. In the range above 1.5 MHz one can observe in higher orders even twenty (for p1) or several percent resonance effect of scattering.

Acknowledgments

This work is supported by Ministry of Science and Higher Education (grant N 518 002 32/0219 and NN 518 388 234)

References

- [1] Wear K., "Frequency dependence of ultrasonic backscatter from human trabecular bone: theory and experiments", *J.Acoust. Soc.Am.*, 106(6),3659-3664, 1999.
- [2] Bossy E., Padilla F., Peyrin F., and Laugier P., "Three-dimensional simulation of ultrasound

propagation through trabecular bone structures measured by synchrotron micro-tomography”, *Phys.Med. Biol.*, vol.50, 5545-5556, 2005.

- [3] Wear K., “Ultrasonic Scattering from Cancellous Bone: A review”, *IEEE Trans. Ultrason. Freq. Contr.*, vol.55,no.7, 1432-1441,2008.
- [4] Brekhovskikh L.M., Godin O.,A., “Acoustics of Layered Media I, ISBN 3-540-51038-9, *Springer-Verlag Berlin Haidelberg New York*, 1-14, 1990.
- [5] Wójcik J., “Conservation of energy and absorption in acoustic fields for linear and nonlinear propagation”, *J.Acoust.Soc.Am.* 104 (5), 2654-2663, November 1998.
- [6] Hosokawa A., “Development of Numerical Cancellous Bone Model for Finite-Difference Time-Domain Simulations of Ultrasound Propagation”, *IEEE Trans. Ultrason. Freq. Contr.*, vol.,55,no. 6, June 2008, 1219-1233.